



Electronic Warfare and Remote Sensing: Radio Frequency (RF) Sensors

Modeling and Experimental Evaluation of Amplitude Error in the Determination of the Angle of Arrival in RWR Sensors

Adônis Virgílio Teixeira Pinto¹, Felipe Streitenberger Ivo², Lucio Pinheiro Amaro², and Renato Machado²¹Second Squadron of the Sixth Aviation Group (2^o/6^o GAV), Anápolis/GO – Brazil²Aeronautics Institute of Technology (ITA), São José dos Campos/SP – Brazil

Article Info

Article History:

Received	29 May	2025
Revised	28 June	2025
Accepted	19 July	2025
Available online	23 September	2025

Keywords:

AOA

RWR

Simulation

Amplitude Comparison Method

Abstract

The Angle of Arrival (AOA) estimated information in Radar Warning Receiver (RWR) sensors using the amplitude comparison method is susceptible to various error sources that can affect its accuracy and precision. Variation in Signal-to-Noise Ratio (SNR), which is directly related to the signal amplitude received by the sensor, is one such factor that can compromise AOA determination. This paper presents a laboratory experiment conducted to assess the AOA error due to variations in SNR. A theoretical analysis is performed, where the SNR is a function of the threat detection angle and the receiver response, including the antenna pattern and position. The experimental analysis validates the theoretical results of the model. Finally, the feasibility of evaluating AOA processing of RWR sensors in a reduced chain configuration through conducted tests is demonstrated, offering an alternative to field or anechoic chamber testing.

E-mail addresses:

adonis.pinto@gmail.com

fivo@ita.br

lucio@ita.br

rmachado@ita.br

1. INTRODUCTION

The determination of the direction of arrival, or Angle of Arrival (AOA), of an electromagnetic signal has been widely used in various applications, such as radar systems, Electronic Warfare (EW) sensors, and Remotely Piloted Aircraft (RPA) [1]–[3]. Depending on the application and the required precision and accuracy of the AOA information, different methods and algorithms are employed for its estimation [4]. Specifically, in aircraft equipped with Radar Warning Receiver (RWR) sensors, two AOA estimation techniques are typically used: the phase comparison technique, which employs interferometry principles to compare the phase of intercepted signals between two or more receiving antennas, and the amplitude comparison technique, commonly referred to by the acronym ACM (Amplitude Comparison-based Monopulse), which compares the signal amplitude, potentially even from a single radar pulse intercepted by two or more receiving antennas [3]–[5].

Due to its simplicity of implementation, high reliability, and shorter signal processing time, the ACM method has become the most widely used in RWR sensors [6], and it is the focus of this paper. However, the ACM method is subject to several sources of error that can compromise the accurate

retrieval of the AOA parameter by the sensor, which is used as an input for signal separation processing [5]. Thus, this article aims to model and analyze, both analytically and experimentally, the impact of the error in AOA estimation in an RWR system using the ACM technique as a function of the variation in the Signal-to-Noise Ratio (SNR), which varies with the emission frequency and direction, considering a simple RWR reception system composed of two adjacent antennas covering a 90-degree angular sector.

Additionally, we propose laboratory-based tests using the Excalibur Radar Threat Emulator from the Electronic Warfare Laboratory to demonstrate the concept and evaluate the system, considering a typical broadband RWR receiver (2–18 GHz). Pulsed signal emissions at three different frequencies — 2.5, 9.0, and 17.5 GHz — were selected. It is assumed that the transmitter (TX) and receiver (RX) are 40 km apart, with the TX's AOA varying at 0°, 22.5°, 45°, 67.5°, and 90° relative to the RX. The SNR was evaluated for each of the two receiving antennas, as well as the AOA error as a function of SNR for the three test frequencies. Finally, the AOA error is also presented considering variations in the 3 dB beamwidth of the receiving antenna, with the following beam directions considered: 90°, 65°, and 115°.

This paper is organized as follows. Section II presents the theoretical foundation for AOA estimation for the type of RWR sensor considered in this study. Section III analyzes the sensor's SNR and the pointing error resulting from its variation. Section IV describes the experimental methodology using Excalibur for conceptual validation. Finally, Section VI concludes the paper.

This work was supported in part by the Center of Competence in Electronic Warfare of the Aeronautics Institute of Technology, National Institute of Science and Technology (INCT-Signals) sponsored by Brazil's National Council for Scientific and Technological Development (CNPq) under grant no. 406517/2022-3, Ministry of Science, Technology and Innovation (MCTI), and by the São Paulo Research Foundation (FAPESP) under grant 20/09838-0 (BIOS—Brazilian Institute of Data Science).

II. AMPLITUDE COMPARISON METHOD FOR AOA ESTIMATION

The determination of AOA by an airborne RWR sensor using the ACM method can be understood from the interception of a signal by an array composed of only two adjacent and orthogonal antennas, typically with a beamwidth (θ_B) of 90° , as shown in Fig. 1. This antenna arrangement is usually designed to provide signal coverage in a 90° azimuth sector of the aircraft. It is worth noting that when this array is expanded with two additional antennas, its coverage capability increases to 360° , a feature common in aircraft equipped with onboard EW systems. Each of the antennas in the RWR is connected to a signal receiver, referred to as RX-1 and RX-2 in Fig. 1.

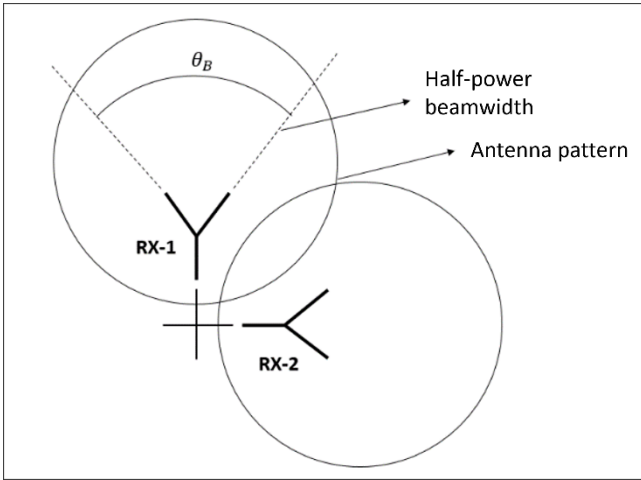


Fig. 1. Two-Antenna Array design for the Amplitude Comparison Method.

Each of the two antennas in the RWR (Fig. 1) is associated with a gain, which is a function of the azimuth angle. The RF power at the output of each antenna can be modeled as a function of the angle at which the signal is intercepted, given by

$$P_i(\theta) = P_{rx} \cdot G_i(\theta), \quad (1)$$

where P_{rx} is the power received considering the effective area of an omnidirectional antenna, $P_i(\theta)$ is the power received at the i -th receiving antenna, and $G_i(\theta)$ is the associated gain.

To measure $G_i(\theta)$, the planar spiral antenna is used as a reference. This type of antenna operates over a wide bandwidth and is commonly used in RWR arrays [9]. It is characterized by its small size and weight, with a beamwidth of about 90° , making it suitable for systems like the one shown in Fig. 1. According to [6], the gain $G_i(\theta)$ can be well modeled by a Gaussian function

$$G_i(\theta) = A_i^2 e^{-k^2(\theta-\alpha)^2}, \quad (2)$$

where A_i is the square root of the antenna's maximum gain at boresight, θ is the azimuth of the emission (i.e., the signal's AOA), α represents the squint angle (the offset between the beamwidth centers), and k^2 varies with the half-power beamwidth θ_B and is given by

$$k^2 = \frac{2,776}{\theta_B^2}. \quad (3)$$

The Gaussian radiation pattern of (2) is illustrated in Fig. 2.

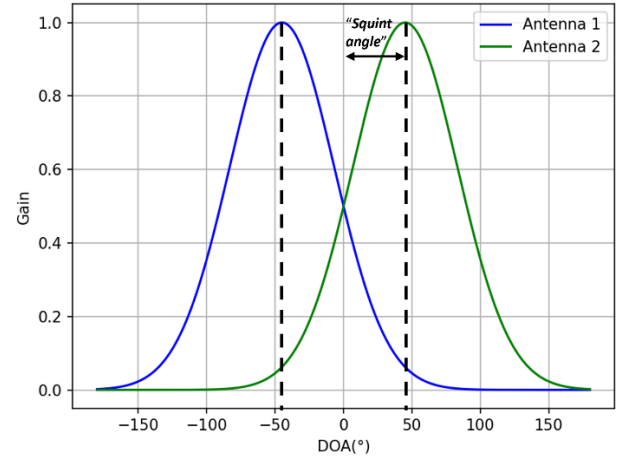


Fig. 2. Gaussian radiation pattern of two adjacent and orthogonal antennas.

By relating the amplitude between the two adjacent antennas in the array, the amplitude ratio is obtained as

$$R(\theta) = \frac{G_1(\theta)}{G_2(\theta)} \quad (4)$$

Substituting (2) into (4) and developing the equations, the AOA value, here referred to as θ , is given by

$$\theta = R(\theta)|_{dB} \left(\frac{\theta_B^2}{48\alpha} \right) \quad (5)$$

Thus, by knowing the half-power beamwidth and the squint angle of the array, the emitter's direction, i.e., the AOA, can be obtained using (5).

III. SIGNAL-TO-NOISE RATIO FOR THE TWO-ANTENNA ARRAY

According to [7], the noise associated with each antenna channel is one of the error sources that affects the amplitude of the signal measured in the respective channel. As per [3], the root mean square (RMS) pointing error of AOA is given by:

$$\sigma_\theta = \frac{\sigma_{R,dB}}{\left[\frac{dR(\theta)|_{dB}}{d(\theta)} \right]}, \quad (6)$$

where $\sigma_{R,dB}$ is the amplitude error due to noise and $\frac{dR(\theta)|_{dB}}{d(\theta)}$ is the amplitude variation with respect to AOA in dB.

The amplitude variation $\sigma_{R_{dB}}$ is associated with the fluctuation of the measured amplitude level relative to the true signal amplitude in the channels of the two adjacent antennas, and can be given by [6]

$$\sigma_{R_{dB}} = 20(\log e) \left(\frac{\Delta A_1}{A_1} - \frac{\Delta A_2}{A_2} \right), \quad (7)$$

where A_1 and A_2 represent the true amplitudes in Channels 1 and 2, and ΔA_1 and ΔA_2 are the amplitude variations in the channels.

Also, according to [3], the SNR can be directly associated with the amplitude fluctuation ΔA presented in (7) and is expressed as

$$\frac{\Delta A}{A} = \frac{1}{\sqrt{2S/N}} \quad (8)$$

Assuming the noise in the two channels is uncorrelated and originates only from thermal noise (N_0), the amplitude error due to noise can be derived from (7) as

$$\sigma_{R_{dB}} = 20(\log e) \left(\frac{1}{2S/N_0} + \frac{1}{2S/N_0} \right)^{1/2} \quad (9)$$

From (1) and (2), the SNR values for each channel at the antenna output can be expressed as a function of the angle θ

$$\begin{aligned} SNR_1(\theta) &= P_{rx} \cdot \left(\frac{A_1^2 e^{[-k^2(\theta-\alpha)^2]}}{N_0} \right) \\ SNR_2(\theta) &= P_{rx} \cdot \left(\frac{A_2^2 e^{[-k^2(\theta+\alpha)^2]}}{N_0} \right) \end{aligned} \quad (10)$$

Analyzing (9), it is observed that SNR is maximized when the values of θ are α and $-\alpha$, respectively. Thus, from (10), it can be seen that when SNR is maximum in one channel, it is minimum in the other, and that the lowest amplitude error associated with SNR occurs at the overlapping angle between the antennas.

Therefore, let us denote the maximum SNR as SNR_0 . Substituting (10) into (9), the error is obtained as

$$\sigma_{R_{dB}} = 20(\log e) \left(\frac{1}{2(SNR_0 e^{[-k^2(\theta-\alpha)^2]})} + \frac{1}{2(SNR_0 e^{[-k^2(\theta+\alpha)^2]})} \right)^{1/2} \quad (11)$$

From (5), the denominator of (6) is fixed since $\frac{dR(\theta)_{dB}}{d(\theta)}$ depends only on θ_B and α , which, in principle, do not vary with the detection angle. Thus, the AOA pointing error can be expressed as

$$\begin{aligned} \sigma_\theta &= 20(\log e) \left[\left(\frac{1}{2(SNR_0 e^{[-k^2(\theta-\alpha)^2]})} + \frac{1}{2(SNR_0 e^{[-k^2(\theta+\alpha)^2]})} \right)^{1/2} \right] \left(\frac{\theta_B^2}{48\alpha} \right) \end{aligned} \quad (12)$$

From the analysis above, it is important to highlight from (12) that the SNR varies with the emission pointing angle relative to the detection system configured with two antennas, and this relationship directly influences the pointing error made by the RWR.

IV. EXPERIMENTAL DEMONSTRATION

The experiments were designed to evaluate the ACM method for determining AOA and to analyze the impact of SNR variation with the pointing angle between the transmitting and receiving antennas. For the experiments, the Excalibur-DRS radar signal emulator was used in conducted mode, meaning that the RF signals were injected directly through coaxial cables into the receiver's front-end. This setup requires the RWR antennas under test to be removed, and the RF cables to be connected directly from the Excalibur to the front-end.

To enhance the reliability of the conducted test, the radiation behavior of the RWR array antennas was experimentally determined in an anechoic chamber. The resulting radiation patterns were imported into the Excalibur's Threat Builder simulation software, which manages the emitter scenarios for the tests.

As shown in Fig. 3, an experimental setup was established to demonstrate the concept for AOA testing and the relationships between SNR and emission direction using a receiving system with two antennas connected to ports 3 and 4 of the Excalibur. In the Threat Builder software, receiving antennas RX-1 and RX-2 were assigned to ports 3 and 4, respectively. Each RF cable used an SMA-to-N adapter and a DC block for analyzer protection. Signal analysis from RX-1 (port 3) was performed using an E4433B spectrum analyzer, while RX-2 (port 4) was connected to an N9035B signal analyzer.

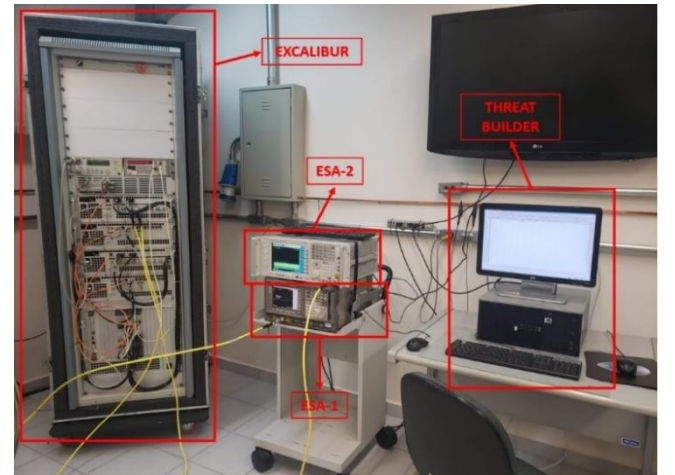


Fig. 3. Experimental setup used for AOA testing.

To carry out the tests, three different radar emitters were configured in Threat Builder, with their parameters presented in Table 1. Although Threat Builder can assign radar signature parameters such as horizontal and vertical antenna patterns, scanning, and other characteristics, a test scenario where these parameters remain fixed was used due to the conceptual nature of the test.

TABLE I. RADAR EMITTERS PROGRAMMED.

Emitter	PW [μ s]	PRI [ms]	PRF [kHz]	F [GHz]	ERP [dBm]
1	10.0	1.0	10	2.5	110
2	10.0	1.0	10	9.0	110
3	10.0	1.0	10	17.5	110

The RX-1 and RX-2 antennas of the RWR were configured with a Gaussian radiation pattern obtained from Equation (2), with a beamwidth θ_B of 90° . The pattern was generated using Python and imported into Threat Builder to simulate the receiver system, considering a squint angle (α) of 45° between antennas spaced 90° apart. The array diagram is shown in Fig. 4.

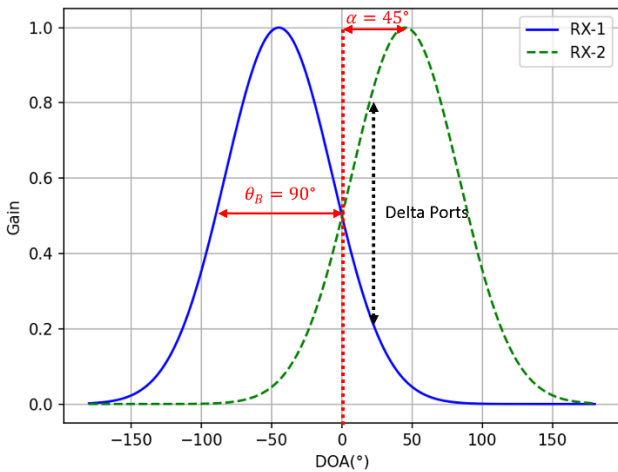


Fig. 4. Radiation diagram of the receiving antenna array.

The transmitting antenna (TX) was positioned 40 km from the receiving array, as illustrated in Fig. 5, and the experiments considered AOA variations of 0° , 22.5° , 45° , 67.5° , and 90° .

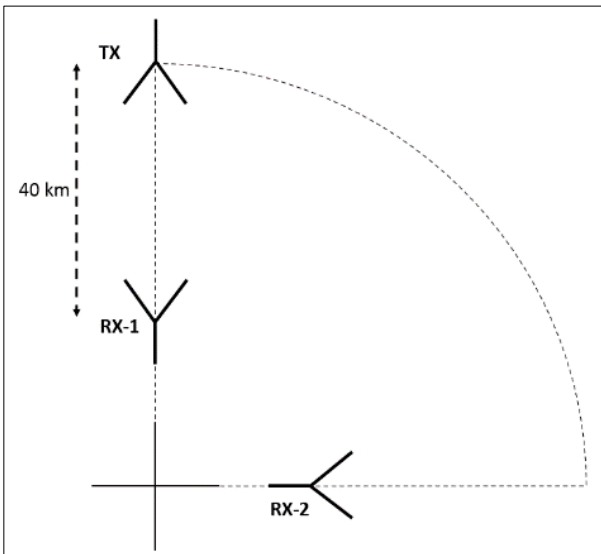


Fig. 5. Rotation test of the TX antenna relative to the array.

V. RESULTS AND ANALYSIS

Within the parameters established for the test, power levels were measured at the spectrum analyzers for signals from ports 3 and 4 for each of the TX antenna's expected AOA values. Using (5), the AOA was calculated for each TX position, considering the emitters listed in Table 1. Based on the measured power values at all TX angles across both channels, the SNR values were evaluated for each AOA of the specified emitters. A Tangential Sensitivity (TSS) of -60 dBm was considered [6]. TSS is defined when the signal value exceeds the noise value by 8 dB [1]. The measured SNR results, obtained using (10), for Emitters 1, 2, and 3 are shown in Figs. 6, 7, and 8.

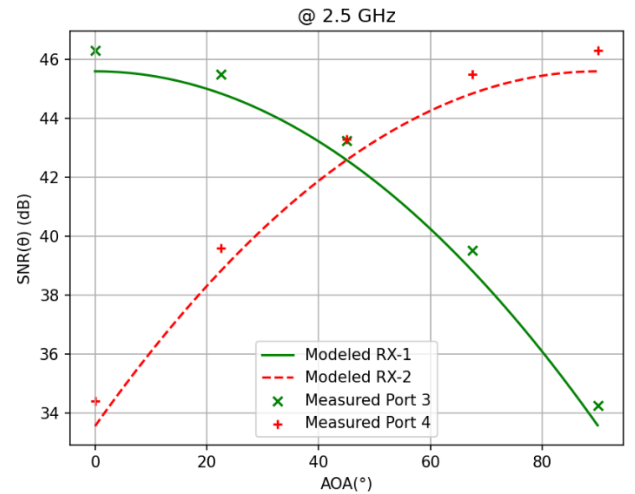


Fig. 6. SNR variation as a function of AOA for Emitter 1.

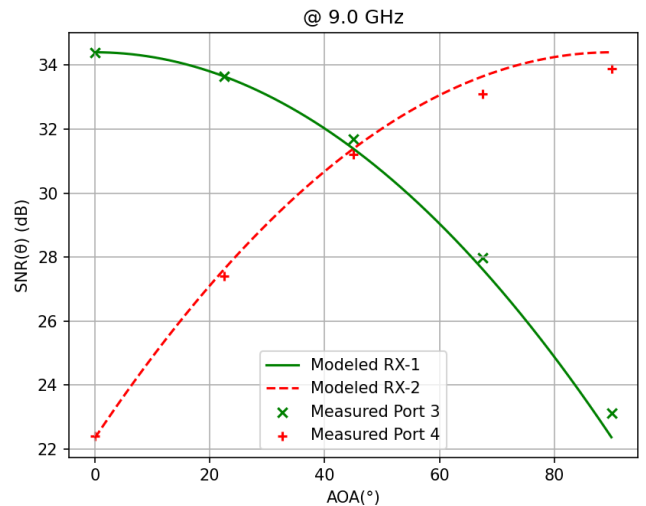


Fig. 7. SNR variation as function of AOA for Emitter 2.

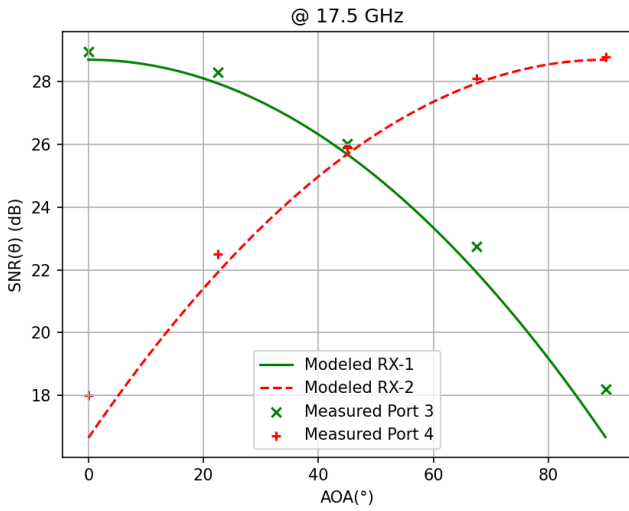


Fig. 8. SNR variation as a function of AOA for Emitter 3.

Based on the AOA values calculated from the experimental data shown in Figs. 6, 7, and 8, only minor variations were observed when compared to the previously modeled theoretical curves. Specifically, the largest amplitude deviation recorded was 1.6 dB, which occurred at port 3 with the antenna positioned at an AOA of 90° for Emitter 3, operating at 17.5 GHz.

In addition, the AOA error σ_θ was comprehensively evaluated as a function of the signal detection angle for all three tested emitters (2.5 GHz, 9.0 GHz, and 17.5 GHz), following the mathematical formulation described in Equation (12). This evaluation employed the SNR values derived from the measurements shown in Figs. 6, 7, and 8, considering a Tangential Sensitivity (TSS) threshold of -60 dBm.

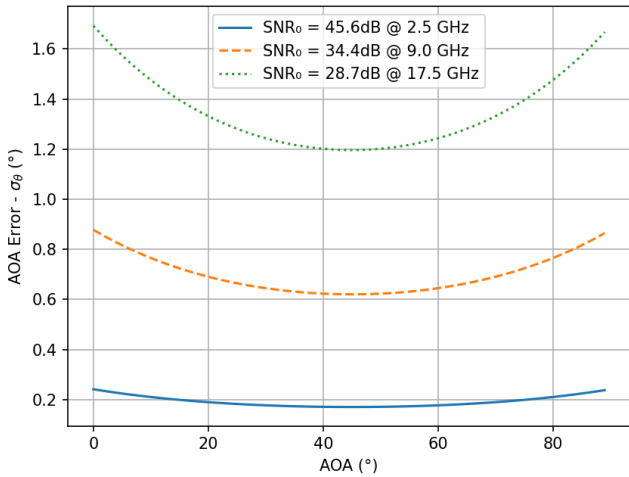


Fig. 9. AOA error σ_θ as a function of AOA for the three evaluated emitters.

From Fig. 9, it can be seen that the AOA error is minimal when the emission is close to the bisector angle between the antennas and maximal as it approaches the array's edges. Additionally, the error increases with frequency, which reduces the signal-to-noise ratio.

The AOA error σ_θ was also analyzed as a function of the emitter's AOA for Emitter 2 (9.0 GHz), but with variations in beamwidth θ_B to 65° and 115°, maintaining a TSS of -60 dBm and considering a SNR_0 of 34.4 dB. The results are presented in Fig. 10.

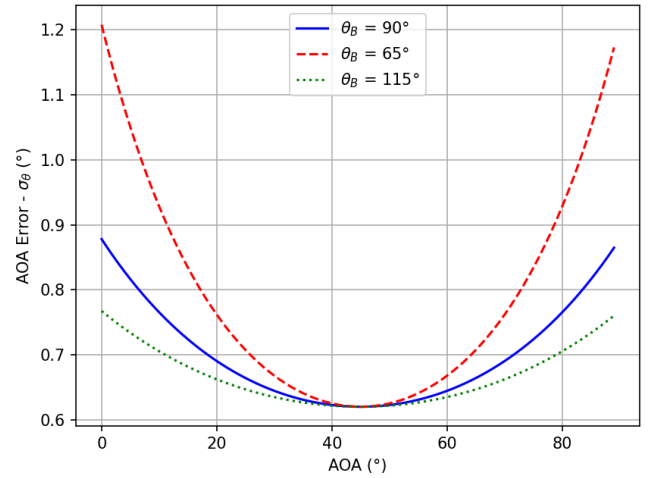


Fig. 10. AOA error as a function of AOA for three different beamwidths.

As shown in Fig. 10 and similar to the results in Fig. 9, the error increases as the emission direction moves away from the bisector angle between the antennas. Additionally, the error increases as the beamwidth decreases. Higher radar signal frequencies result in narrower antenna beamwidths. Therefore, AOA information is subject to higher or lower errors depending on the emission frequency.

It is important to note that this analysis considered a fixed squint angle, disregarding variations in beamwidth.

VI. CONCLUSION

The amplitude comparison method for AOA measurement can have a direct influence on the performance of RWR systems, including their ability to distinguish radar signal sources that are spatially separated but otherwise identical. In this context, this study aimed to analytically quantify the contribution of signal-to-noise ratio (SNR) to AOA error using a simple model that considers a 90-degree sector covered by two adjacent antennas. Laboratory tests were also conducted to demonstrate the concept and measure error variation due to changes in different system parameters.

Based on the proposed model and the tests conducted, it was found that the SNR in AOA determination using the ACM method in an RWR system varies with the direction from which the signal originates.

Additionally, it was observed that the variation of SNR with the emission AOA compromises the accuracy of the AOA measurement. Therefore, in RWR systems whose primary function is to indicate the emitter's position, the angular direction relative to the receiving system directly affects the AOA estimation using the ACM method. The error tends to be greater when the signal approaches the antennas' boresight and smaller near the bisector angle between the antennas.

Similarly, when analyzing the trade-off between beamwidth and AOA error, it was noted that for the same signal AOA, the error increases as the half-power beamwidth decreases, as well as with the increase in error due to lower SNR. Thus, variations in beamwidth—potentially caused by frequency changes—can also lead to errors in AOA estimation.

It is worth emphasizing, however, that the AOA errors studied in this model are small for an RWR sensor, but they are cumulative and were shown to be nonlinear with respect to the angle of arrival. Furthermore, in the case study analyzed in this paper, the effective radiated power was fixed at a high value, which is higher than what might be encountered in real-world scenarios, where lower values may further degrade the SNR. Moreover, the emissions may also be subject to other detection effects not incorporated into the model, such as multipath.

Finally, the laboratory experiments demonstrated that the Excalibur-DRS system can be used to test AOA performance, including error sources, for evaluating a real RWR sensor arranged in a reduced chain.

REFERENCES

- [1] J. B. Tsui, *Microwave Receivers With EW Applications*. Scitech Publishing, 2005.
- [2] M. Zuo and S. Xie, “A novel DOA estimation method for an antenna array under strong interference,” *EURASIP J Adv Signal Process*, vol. 2022, no. 1, Dec. 2022, doi: 10.1186/s13634-022-00930-y.
- [3] R. G. Wiley, *ELINT The Interception and Analysis of Radar Signals*. Norwood, MA: Artech House, 2006.
- [4] E. Yan *et al.*, “Improving accuracy of an amplitude comparison-based direction-finding system by neural network optimization”, *IEEE Access*, vol. 8, p. 169688–169700, 2020, doi: 10.1109/ACCESS.2020.3024031.
- [5] S. Robertson, *Practical ESM Analysis*. Norwood, MA: Artech House, 2019.
- [6] A. de Martino, *Introduction to modern EW systems*, 2^o ed. Norwood, MA: Artech House, 2018.
- [7] M. F. Iqbal, Z. Khalid, M. Zahid, e A. Abdullah, “Accuracy improvement in amplitude comparison-based passive direction finding systems by adaptive squint selection”, *IET Radar, Sonar and Navigation*, vol. 14, n^o 5, p. 662–668, maio 2020, doi: 10.1049/iet-rsn.2019.0465.
- [8] F. S. Ivo, P. C. da S. Euphrásio, A. P. Gonçalves, R. J. Zandoná, L. de A. Faria, e O. L. Coutinho, “Operação remota do sistema gerador de cenários de guerra eletrônica DRS-Excalibur associada à transmissão de sinais radar em fibra óptica”, *Spectrum-Aplicações Operacionais em Áreas de Defesa*, vol. 1, São José dos Campos, SP, p. 4–11, set. 30, 2021.
- [9] A. B. Constantine, *Antenna Theory: Analysis and Design*, 2^o ed. New York - NY: John Wiley & Sons, 1997.